HHS Public Access

Author manuscript

Bioorg Med Chem. Author manuscript; available in PMC 2020 October 15.

Published in final edited form as:

Bioorg Med Chem. 2013 May 01; 21(9): 2623–2634. doi:10.1016/j.bmc.2013.02.020.

Development of cyclic peptomer inhibitors targeting the polo-box domain of polo-like kinase 1

Ravichandran N. Murugan[a,†], **Jung-Eun Park**[b,†], **Dan Lim**[c], **Mija Ahn**[a], **Chaejoon Cheong**[a], **Taeho Kwon**[b,d,e,f], **Ky-Youb Nam**[g], **Sun Ho Choi**[b,h], **Bo Yeon Kim**[f], **Do-Young Yoon**[e], **Michael B. Yaffe**[c], **Dae-Yeul Yu**[d], **Kyung S. Lee**[b,*], **Jeong Kyu Bang**[a,*]

[a]Division of Magnetic Resonance, Korea Basic Science Institute, Ochang, Chung-Buk 363-883, Cheongwon, Republic of Korea

[b]Laboratory of Metabolism, Center for Cancer Research, National Cancer Institute, National Institutes of Health, 9000 Rockville Pike, Building 37, Room 3118, Bethesda, MD 20892, United States

[c]Department of Biology and Biological Engineering, Center for Cancer Research, Massachusetts Institute of Technology, Cambridge, MA 02139, United States

[d]Aging Research Center, Korea Research Institute of Bioscience and Biotechnology, Daejeon 305-806, Republic of Korea

[e]Department of Bioscience and Biotechnology, Bio/Molecular Informatics Center, Konkuk University, Seoul 143-701, Republic of Korea

[f]World Class Institute, Korea Research Institute of Bioscience and Biotechnology, Ochang, Republic of Korea

[g]Bioinformatics and Molecular Design Research Center, B128A Yonsei University Research Complex, Shinchon-dong, Seoul 120-749, Republic of Korea

[h]Dong-A Pharmaceutical Co., Ltd., Research Laboratories, Yongin 449-905, Republic of Korea

Abstract

The polo-box domain (PBD) of polo-like kinase 1 (Plk1) is essentially required for the function of Plk1 in cell proliferation. The availability of the phosphopeptide-binding pocket on PBD provides a unique opportunity to develop novel protein–protein interaction inhibitors. Recent identification of a minimal 5-residue-long phosphopeptide, PLHSpT, as a Plk1 PBD-specific ligand has led to the development of several peptide-based inhibitors, but none of them is cyclic peptide. Through the combination of single-peptoid mimics and thio-ether bridged cyclization, we successfully demonstrated for the first time two cyclic peptomers, PL-116 and PL-120, dramatically improved

*Corresponding authors. Tel.: +1 301 496 9635; fax: +1 301 496 8419 (K.S.L.); tel.: +82 43 240 5023; fax: +82 43 240 5059 (J.K.B.). kyunglee@mail.nih.gov (K.S. Lee), bangjk@kbsi.re.kr (J.K. Bang).

†These authors contributed equally to this work.

Supplementary data

Supplementary data (additional figures and table that corresponds to the modeling and Plk1 PBD-binding assay studies, IC_{50} values and compounds structures) associated with this article can be found, in the online version, at http://dx.doi.org/10.1016/j.bmc.2013.02.020.

the binding affinity without losing mono-specificity against Plk1 PBD in comparison with the linear parental peptide, PLHSpT. These cyclic peptomers could serve as promising templates for future drug designs to inhibit Plk1 PBD.

Keywords

Polo-box domain (PBD); Cyclic peptomers; Kinase inhibitors; Solid phase peptide synthesis

1. Introduction

Protein kinases comprise a large family of enzymes that phosphorylate specific protein substrates using the terminal phosphoryl group of adenosine triphosphate (ATP). A large body of evidence suggests that phosphorylation frequently alters normal cellular functions, such as cell metabolism and proliferation, which are associated with various disease states in humans.[1] As a result, protein kinases constitute the second largest group of attractive drug targets behind membrane-associated receptors, including G protein-coupled receptors. Over the years, various attempts have been made to generate potent inhibitors against clinically important kinases by inhibiting their catalytic activity. However, largely due to a significant level of structural similarities among the ATP-binding sites of the catalytic domains, these efforts have greatly suffered from a lack of target specificity. Therefore, to achieve a high degree of specific inhibition, while avoiding the competition with a high concentration of intracellular ATP, targeting specific protein–protein interaction has emerged as an attractive alternative strategy.[2]

Polo-like kinase 1 (Plk1) is a member of the polo-like kinases family (Plk1–5 in humans; collectively termed Plks) that plays a critical role in regulating mitotic progression and cell proliferation. Plk1 is overexpressed in a broad spectrum of human cancers. A elevated Plk1 activity is thought to promote tumorigenesis, and is considered an attractive anti-cancer drug target. On the other hand, Plk2 and Plk3 appear to play a role in checkpoint-mediated cell cycle arrest to maintain genetic stability and prevent oncogenic transformation.[3] Therefore, specific inhibition of Plk1, but not Plk2 or Plk3, could be important for anti-Plk1 cancer therapy.[4]

Like other Plks, Plk1 contains a characteristic polo-box domain (PBD) within its C-terminal non-catalytic region. A large body of evidence suggests that PBD interacts with phosphoserine/phosphothreonine (pS/pT)-containing motifs and directs the N-terminal catalytic activity to specific subcellular localizations.[3] Extensive studies on the interaction between Plk1 and its centromere/kinetochore-associated binding target, called polo-box-interacting protein 1 (PBIP1),[5] led to the discovery of a 5-residue-long sequence, PLHSpT (residues 74–78 of PBIP1), as a minimal peptide motif that binds to Plk1 PBD with high affinity and specificity.[6] Since then, several attempts have been made to generate the linear PLHSpT derivatives with enhanced anti-Plk1 PBD except the one to synthesize the cyclic peptides with improved binding affinity.[7–11]

In this study, using PLHSpT-based peptide–peptoid hybrids (peptomers), we generated a group of cyclized peptomer derivatives that potently inhibit Plk1 PBD with a high degree of

selectivity. Given the advantages offered by cyclized peptomers in terms of binding affinity and mono-specificity, these inhibitors may serve as a template for developing clinically valuable anti-Plk1 inhibitors. In addition, our study reveals for the first time structural elements that are crucial to providing cyclic constraints for thioether-bridged cyclic peptomers and to achieving potent inhibition of Plk1 PBD. The structure-based approach described here may provide valuable insights into the future design of selective small-molecule Plk1 inhibitors.

2. Results and discussion

2.1. Structure-guided design of cyclic peptomers

To design conformationally constrained cyclic peptomers that might best mimic the phosphopeptide-binding pocket of Plk1 PBD, we first closely examined the binding nature of Plk1 PBD in complex with phosphopeptide ligands. In particular, analysis of the structure of Plk1 PBD in complex with PLHSpT (PDB ID: 3HIK) revealed that the C-terminal pT residue is essential for high-affinity binding, while the N-terminal Pro residue is crucial in conferring the specificity by docking its side chain into a hydrophobic core surrounded by the Trp414, Phe535, and Arg516 residues. The specificity appears to stem from the fact that the N-terminal Pro residue fails to interact with the PBDs of Plk2 and Plk3, which possess the Lys and Tyr residues at positions corresponding to the Arg516 and Phe535 residues, respectively, in Plk1 PBD.[6] In addition, the ‘broader’ pyrrolidine-binding region of PBD surrounded by Trp414 and Phe535 suggests the presence of an unexplored binding surface on PBD (Scheme 1).

By exploiting the broader pyrrolidine-binding pocket described above, we generated cyclic peptomer inhibitors against Plk1 PBD that exhibit an improved binding affinity while retaining Plk1 PBD specificity. To obtain diverse cyclic derivatives, a library was made by employing both head-to-tail and side chain-to-tail cyclization methods (Figs. 1 and 3). These methods allowed us to achieve skeletal diversity by forming amide-, thioether-, or triazole-bridged cyclic analogues. To explore the above broader pyrrolidine-binding region surrounded by the Trp414 and Phe535 residues of Plk1 PBD, we utilized the pi–pi mediating functional groups to replace the N-terminal Pro of PLHSpT.[12] This was accomplished by substituting the Pro-4 residue with a peptoid backbone via a submonomer method[13] that utilizes a vast number of aromatic amines as starting materials, mimicking the side chains of amino acid residues. This method eventually led to the generation of diverse (aromatic, charge, size, heteroaryl, length, etc.) structural scaffolds that may target the broader pyrrolidine binding region.[14]

2.2. Peptide synthesis and preliminary evaluation

All the linear precursors were prepared with the standard Fmoc-based solid-phase peptide protocol using either Rink amide or Chloro-trityl resin. Our first-phase derivatization efforts for cyclic peptides or peptomer (Figs. 1 and 3) were divided into four categories. The first category contained the amide-bridged cyclic peptides (PL-1 to PL-3) either bearing all the key residues of the parent PLHSpT peptide (PL-1), bearing Gly in replacement of Pro (PL-2), or lacking the Pro residue (PL-3). To facilitate selective cleavage and amide

cyclization on resin, the Fmoc-Glu-OAll amino acid was attached to Rink amide resin via its side-chain acid functionality, followed by the sequential attachment of the Fmoc-protected amino acids on the growing chain (PL-1 to PL-3). Subsequent deprotection of the allyl group using $Pd(PPh_3)_4$, followed by head-to-tail cyclization in the presence of a peptide-coupling agent, PyBrOP, yielded the cyclic peptides PL-1 to PL-3. For the second thioether-bridged category, Fmoc-Cys(Trt)-OH, instead of Fmoc-Glu-OAll, was attached to the C-terminus of the 5-mer LHSpTA (PL-4) or PLHSpT (PL-5) and acylation was performed at the N-terminus using bromoacetic acid in the presence of DIC (*N,N*′-Diisopropylcarbamide) to facilitate the side chain-to-tail cyclization. Our third category contained a single triazole-bridged cyclic peptide (PL-50) that was generated through the condensation (i.e., 1,3-dipolar cycloaddition reaction) between the N-terminal 5-azidopropanoic acid (Scheme 3) and the C-terminal propargylamine of the linear peptide in the presence of CuI and 2,6-lutidine. Finally, for the fourth category, we utilized the power of peptoid mimics to conduct an extensive structure–activity relationship (SAR) investigation on the chosen bioactive cyclic scaffold from the above three different categories (amide, thioether, and triazole-bridged peptides). The competitive inhibitory activity of the above cyclic peptides was evaluated using the ELISA-based Plk1 PBD inhibition assay described previously.[6]

From the results of the cyclic peptide derivatives (PL-1 to PL-5 and PL-50; see Fig. 1), we found that the thioether-bridged cyclic analogue PL-5 (IC_{50} = 9.80 μM) inhibited Plk1 PBD more efficiently than other cyclized peptides (PL-1–PL-4 and PL-50) (Fig. 2a). Molecular modeling studies on PL-5 suggested that the pThr residue of PL-5 coordinated with the two side chains of the His538 and Lys540 residues through ionic interactions, and the N-terminal Pro residue interacted with the Arg516 residue through an H-bonding interaction (Fig. 2b). In contrast to PL-5, both amide- and triazole-bridged cyclic peptides (PL-1–PL-3 and PL-50, respectively) failed to dock into the phosphopeptide-binding region of Plk1 PBD with the electrostatic (pThr) and hydrophobic (Pro) inter-action-mediating residues (Supplementary Fig. S1), resulting in the loss of inhibitory activity. Therefore, we utilized the thioether scaffold in our fourth category as a core skeleton for further modifications (Fig. 3).

Using the thioether template (Supplementary Scheme S1), we generated cyclic peptide or peptomers that either containing the key LHSpTC residues (PL-12), N-shifted Leu (*N*eu) substitution on PL-12 (PL-11, Scheme 2), different lengths of the aromatic substituted side chains (PL-7, 8, and 9) diverse electronegative atoms (PL-6, 10, and 22), or aromatic groups (PL-8, 21, and 23). Similarly extensive structural variation was also made using double-peptoid mimics of cyclic peptomers (PL-13 to PL-20, Fig. 3). From these efforts, we obtained eight confirmed hits (7–10, 15, 19, 22, and 23) when compared to the parental PLHSpT peptide (IC_{50} = 32.03 μM) (Fig. 4 and Supplementary Table S1). As expected, cyclic peptomers, PL-11 and PL-12, lacking the Pro residue at their N-termini failed to inhibit Plk1 PBD. Among the cyclic peptomers from the first phase of derivatization, PL-23 (IC_{50} = 8.50 μM; Supplementary Table S1) containing an indole moiety showed the highest binding affinity (Fig. 4). Additionally, a gain in the inhibitory activity of PL-7 was revealed by testing alkylated phenyl groups with different lengths of methylene spacers (PL-7, PL-8, and PL-9; Figs. 3 and 4a). Interestingly, the two most potent cyclic peptomers, PL-23 and PL-7, closely resembled each other in terms of possessing aromaticity at the Pro-4 position. These findings support our hypothesis that the occupation of the border pyrrolidine-binding

region using the pi–pi stacking interacting moieties is important to improve the binding affinity, and further suggest that optimizing both carbon tethering and aromaticity is critical to achieving a potent inhibition against Plk1 PBD.

Another interesting finding was that single peptoid–substituted cyclic peptomers were more active than double peptoid–substituted peptomers (compare PL-23 with PL-15 and PL-10 with PL-16). This observation supports the argument that, in comparison to highly flexible double peptoid–substituted derivatives, single peptoid–substituted derivatives may provide optimum flexibility, which is important for assuming a favorable conformation for Plk1 PBD inhibition.[15] The SAR analyses also suggested that a free OH-substituted aromatic derivative (PL-22) has greater inhibitory activity than a chloro-substituted cyclic peptomer (PL-6, Fig. 3). Among the cyclic peptomers containing two peptoids, PL-20 exhibited a significantly increased level of Plk1 PBD inhibition, whereas PL-13 displayed inhibitory activity similar to PLHSpT (Fig. 4b). This binding difference led us to speculate that the methyl substitution in PL-13 may have prevented its phenyl group from being properly positioned to have pi–pi interactions with the Trp414 and Phe535 residues. Since PL-23 showed the highest binding affinity, we performed a more detailed SAR study with PL-28, PL-29, and PL-30. To our surprise, PL-28, bearing Trp in replacement of *N*Trp, significantly lost its binding affinity in comparison to cyclic peptomer PL-23 (Supplementary Fig. S2a). This finding suggests that conferring optimum flexibility using peptoid mimics is crucial to attaining potent inhibition of Plk1 PBD. Additionally, deleting either Leu (PL-29) or both His and Leu (PL-30) from PL-23 dramatically decreased the binding affinity (Supplementary Fig. S2a). Taken together, our results provided above show that the broader pyrrolidine-binding region can interact with diverse aromatic groups, and this interaction can provide additional affinity to Plk1 PBD binding.

2.3. Second-phase library design, synthesis, and screening

On the basis of our first phase of cyclic peptomer derivatization, we found that both the four methylene linker (PL-7) and indole group (PL-23) are important for Plk1 PBD binding (Fig. 4). Hence, for the second phase of derivatization, we decided to further diversify the Pro position (Fig. 5a) to try to determine other elements critical for the binding of cyclic peptomers. We observed that compound PL-24, bearing an indole group with a four methylene spacer, exhibited an approximately twofold increase in Plk1 PBD binding affinity (IC_{50} = 4.75 μM) in comparison to that of the parent cyclic peptide (PL-23, IC_{50} = 8.50 μM) (Fig. 5b, Supplementary Fig. S2a and Supplementary Table S1). This finding suggests that lengthening the methylene spacer from two (PL-23) to four (PL-24, Scheme 4) is likely important for enhancing Plk1 PBD binding.

Next, we investigated whether the acetylation of the indole ring in PL-24 (PL-113) influences its inhibitory activity against Plk1 PBD. We observed that the activity of PL-113 was very similar to that of PL-24, although PL-113 exhibited a much higher synthetic yield than PL-24. Intriguingly, however, lengthening the carbon tethering from four (PL-113) to six (PL-119) or seven (PL-116) substantially improved Plk1 PBD inhibitory activity (Scheme 4 and Supplementary Fig. S2b). Notably, PL-116, containing the longest methylene spacer conjugated to the acetylated indole group, displayed one of the highest inhibitory

activities (IC_{50} = 2.56 μM) against Plk1 PBD, which was 3.3-fold higher than the parental cyclic peptide PL-23 (IC_{50} = 8.50 μM) (Fig. 5b and Supplementary Table S1). A recent study showed that the $C_6H_5(CH_2)_8$–moiety conjugated to the His residue of PLHSpT conferred a substantially increased binding affinity to Plk1 PBD by tightly binding to the Tyr-rich hydrophobic channel residing across the well-characterized SpT dipeptide-binding pocket.[7] Therefore, we investigated whether adding the $C_6H_5(CH_2)_8$– moiety (Scheme 5) enhances the ability of PL-116 to bind to Plk1 PBD as well. Remarkably, the resulting compound, PL-120, exhibited approximately 2.5-fold lower IC_{50} value (IC_{50} = 1.08 μM; Supplementary Table S1) than PL-116 (IC_{50} = 2.56 μM). These findings suggest that both the peptoid moiety and the $C_6H_5(CH_2)_8$-conjugated His adduct are critical for the binding of PL-120 to Plk1 PBD (Fig. 5b).

2.4. Impact on selectivity

Restricting an inhibitor's conformation to a structure recognized by a target protein(s) is thought to increase potency by lowering the entropic barrier to complex formation. This restriction could also potentially enhance the specificity of the inhibitor by limiting its interaction modes with the target protein.[16] To examine the binding specificity of PL-116 and PL-120 in comparison to that of parent PLHSpT, we carried out a specificity test for these derivatives against PBDs from closely related Plk1, 2, and 3. Plk4 PBD was not included because of the distinct binding nature of this protein.[17] The results showed that both of these cyclic peptomers exhibited mono-specificity against Plk1 PBD (Fig. 6), even though their binding affinities were ~30-fold higher than parent PLHSpT. To the best of our knowledge, PL-116 and PL-120 were the first cyclic peptomers to exhibit isoform-selective inhibition against Plk1 PBD.

2.5. Modeling studies on Plk1 PBD:ligand complex

To better understand the binding nature of two selected cyclic peptomers, PL-116 and PL-120, in complex with Plk1 PBD, we used the previously reported crystal structure of the Plk1 PBD–PLHSpT complex[6] as a template and performed molecular dynamics simulation studies. These modeling studies suggested that the acetylated indole peptoid fragment was engaged in the cation–pi interaction with the Arg579 residue present in the extended pyrrolidine binding region surrounded by Phe534, Arg579, and Tyr582 residues. In addition, a strong hydrogen bond could be formed between the amide bond close to the indole ring and the backbone carbonyl group of Arg518 (Fig. 7a and Supplementary Fig. S3a). This model also suggested that the peptoid fragment from PL-116 failed to fit into the Tyr-rich hydrophobic channel, which was previously disclosed by Burke and co-workers.[7] These predictions are consistent with the molecular models obtained with PL-120 (Fig. 7b and Supplementary Fig. S3b) that comprises two discrete binding elements for the Plk1 PBD—the His-2-dependent Tyr-rich hydrophobic channel and the Pro-4-dependent hydrophobic region.

In this study, we synthesized two cyclic peptomers, PL-116 and PL-120, containing either an indole fragment alone as a peptoid mimic (PL-116) or both an indole fragment and the previously described His[7] (PL-120), and compared their potency with that of the parental linear PLHSpT in vitro. The cyclic peptomer, PL-120, bearing two pharmacophoric groups

binding to the opposite sides of the PLHSpT backbone, exhibited a twofold increase in Plk1 PBD inhibition activity over PL-116. Single peptoid mimics and thioether-bridged cyclization appeared to be the two elements that are critical to imposing a highly potent inhibition against Plk1 PBD. We successfully demonstrated that our two mono-specific cyclic peptomers, PL-116 and PL-120, dramatically improved binding affinity (~30 times) when compared with the linear parental peptide, PLHSpT. These cyclic peptomers could serve as promising templates for future drug designs to inhibit Plk1 PBD.

3. Experimental

3.1. General experimental

All reactions requiring anhydrous conditions were conducted in flame-dried reaction vessels under a positive pressure of Ar. All reagents were purchased from Aldrich Company. For the chromatography analysis, HPLC-grade solvents such as hexane, ethyl acetate, methylene chloride, and methanol were used. Thin-layer chromatography (TLC) was performed on analytical Merck silica gel 60 F254, and were visualized under UV light first, then by using a ninhydrin solution (approx. 0.1% w/v in ethanol) followed by warming. Flash chromatography was performed on Merck silica gel 60 (230–400 mesh). NMR spectra were recorded on a Bruker Avance 300 spectrometer at 300 and 75.5 MHz for ^{1}H and ^{13}C, respectively, with $CDCl_3$. All organic extracts were dried using magnesium sulfate and concentrated under reduced pressure by rotary evaporation. Reverse-phase HPLC analysis (RP-HPLC) was carried out on an Agilent HPLC system equipped with a C_{18} analytical column (250 × 10 mm, 5 μ). Two different linear gradients of 0.05% aq TFA (eluent A) and 0.05% TFA in CH_3CN (eluent B) were used with a flow rate of 2.5 mL/min at 25 °C.

Amines (6–10, 13, 15, 18, and 22) were purchased from Sigma–Aldrich. Fmoc-*NLeu*-OH,[18] 5-azidopropanoic acid,[19] amines[20] (24, 113, 116 & 119), and Fmoc-[*N(π)*-$(CH_2)_8C_6H_5$]-His-OH[21] were prepared according to the indicated literature procedures (Supplementary Fig. S4)

3.2. General procedures for peptide synthesis

All peptides were prepared by Fmoc SPPS methods using Rink amide or Chloro-trityl resin with an initial loading of 0.61 mmol/g, unless otherwise noted. Fmoc-Thr(PO(OBzl)OH)-OH and other Fmoc(fluorenylmethoxycarbonyl) protected amino acids were purchased from Novabiochem. Resins were swollen in *N,N′* -dimethylforamide (DMF) for 45 min prior to synthesis. For sequence extension, the Fmoc-protected amino acid (5.0 equiv) was activated by treatment with 1-*O*-benzotriazole-*N,N,N′ ,N′* -tetramethyl-uronium-hexafluoro-phosphate (HBTU) (5.0 equiv) and hydroxy-benzotriazole (HOBt) (5.0 equiv) in DMF (2 mL) for 2 min. This solution was added to the free amine on resin along with *N,N*-diisopropylethylamine (10.0 equiv) and the coupling reaction was allowed to proceed for 1 h with Vortex stirring. After washing with DMF, Fmoc deprotection was achieved with 20% piperidine in DMF (1 × 10 min, 2 × 3 min). The resin was washed once again, and the process was repeated for the next amino acid and finally the resin was washed with DMF, methanol, dichloromethane and ether, and then dried under vacuum.

3.3. Peptide cleavage

Linear peptides were cleaved from the resin with 5% triisopropylsilane (TIS) and 5% H_2O in trifluoroacetic acid (TFA, approximately 2 mL of TFA per 100 mg of resin) for 2 h. The cleavage mixture was mixed with cold ether to precipitate the peptide and then filtered. The filtrate was washed with cold ether, and the peptide was used for further cyclization step.

3.4. Analytical HPLC conditions

The purities of peptides were determined by using either Phenomenex column (C_{18}, 250 × 4.60 mm, 5 μ) with a linear gradient from 10% aqueous acetonitrile (0.05% trifluoroacetic acid) to 90% acetonitrile (0.05% trifluoroacetic acid) over 30 min at a flow rate of 1.0 mL/min, detection at 230 nm or Vydac HPLC columns (C_{18}, 250 × 10 mm, 5 μ) with a linear gradient from 10% aqueous acetonitrile (0.05% trifluoroacetic acid) to 90% acetonitrile (0.05% trifluoroacetic acid) over 30 min at a flow rate of 2.5 mL/min, detection at 230 nm.

3.5. Peptide synthesis using Fmoc-Glu-OAll

Peptides were synthesized by a three-step synthesis method in a 0.061 mmol scale with Rink Amide Resin to produce an amide C-terminus using manual solid phase peptide synthesis. An example for synthesizing designed cyclo [PLHSpTQ], PL-1 was shown below. Standard Fmoc strategy as described above was used in Step 1. Removal of the Allyl group in Step 2 was performed manually by 2.0 equiv of $Pd(PPh_3)_4$ in a mixture solvent of AcOH/$CHCl_3$/NEM (2/37/1) for 12 h, followed by washing using MeOH, DCM and ether. Then, 20% piperidine in DMF was transferred to the reaction vessel to remove the Fmoc. Peptides were cleaved by TFA at room temperature for 2 h, followed by filtration, precipitation in cold ether, centrifugation, and drying under vacuum. The resulting linear peptides were cyclized in Step 3 using 5.0 equiv of PyBrop in DIEA at 50 °C. Crude peptides were further purified by reverse phase-HPLC.

3.5.1. First phase cyclic peptide or peptomer derivatives–amide-bridged cyclic peptides

Cyclic peptide, PL-1.: Synthesis on 0.062 mmol scale. Purity of crude product 43% (C_{18} RP-HPLC). Yield after purification: 11 mg, 24%; white powder; RP-HPLC t_R = 17.07 (linear gradient, 0–70% B, 30 min); MS (MALDI-TOF) m/z = 745.8 $[M+H]^+$.

Cyclic peptide, PL-2.: Synthesis on 0.058 mmol scale. Purity of crude product 42% (C_{18} RP-HPLC). Yield after purification: 9 mg, 22%; white powder; RP-HPLC t_R = 13.75 (linear gradient, 0–70% B, 30 min); MS (MALDI-TOF) m/z = 702.1 [M − 1].

Cyclic peptide, PL-3.: Synthesis on 0.062 mmol scale. Purity of crude product 11% (C_{18} RP-HPLC). Yield after purification: 2 mg, 5%; white powder; RP-HPLC t_R = 13.53 (linear gradient, 0–70% B, 30 min); MS (MALDI-TOF) m/z = 647.52 $[M+H]^+$.

3.6. Peptide synthesis by thioether-bridged bond formation

As mentioned above, using Fmoc protection strategy, the linear side-chain protected peptide was synthesized on the Rink amide resin (0.61 mmol/g) coupled with the respective amino

acids, and the Fmoc group in the N-terminal of the resin-bound protected peptide was removed with 20% piperidine/DMF. Then, the resin-bound protected peptide was N-terminally bromoacetylated by $(BrCH_2CO)_2O$ which was prepared by mixing 10.0 equiv of $BrCH_2COOH$ and 5.0 equiv of DIC for 3 h at rt. The peptide (0.061 mmol) was cleaved from the resin and dissolved in 10 mL of water/CH_3CN (1:1) mixture followed by the dropwise addition of triethylamine to adjust the pH 8–9, repeatedly. Under the basic conditions the N-bromoacetylated linear peptide cyclized spontaneously by intramolecular nucleophilic displacement of the bromo group by cysteine thiol. The cyclization process was monitored by HPLC. After 1 h at rt, the solution was acidified with 30% AcOH aq solution and lyophilized. The product was purified by RP-HPLC.

In case of peptoid substitution in cyclic peptomers, after the bromoacetylation step, the linear peptides on resin was coupled with the respective primary amine aromatic derivatives (Supplementary Fig. S4). Then, one more bromoacetylation step was carried out on the secondary amine in order to facilitate the cyclization in solution phase using cysteine thiol.

3.6.1. Thioether-bridged cyclic peptides or peptomers having single peptoid

Cyclic peptide, PL-4.: Synthesis on 0.061 mmol scale. Purity of crude product 25% (C_{18} RP-HPLC). Yield after purification: 5.5 mg, 12%; white powder; RP-HPLC t_R = 15.52 (linear gradient, 0–70% B, 30 min); MS (MALDI-TOF) m/z = 750.26 $[M+H]^+$.

Cyclic peptide, PL-5.: Synthesis on 0.061 mmol scale. Purity of crude product 23% (C_{18} RP-HPLC). Yield after purification: 5.2 mg, 11%; white powder; RP-HPLC t_R = 15.52 (linear gradient, 0–70% B, 30 min); MS (MALDI-TOF) m/z = 775.67 [M].

Cyclic peptomer, PL-6.: Synthesis on 0.061 mmol scale. Purity of crude product 44% (C_{18} RP-HPLC). Yield after purification: 11.2 mg, 21%; white powder; RP-HPLC t_R = 18.25 (linear gradient, 10–90% B, 30 min); MS (MALDI-TOF) m/z = 874.91 $[M+H]^+$.

Cyclic peptomer, PL-7.: Synthesis on 0.055 mmol scale. Purity of crude product 21% (C_{18} RP-HPLC). Yield after purification: 5.2 mg, 11%; white powder; RP-HPLC t_R = 18.97 (linear gradient, 10–90% B, 30 min); MS (MALDI-TOF) m/z = 868.51 $[M+H]^+$.

Cyclic peptomer, PL-8.: Synthesis on 0.061 mmol scale. Purity of crude product 30.1% (C_{18} RP-HPLC). Yield after purification: 7.2 mg, 14%; white powder; RP-HPLC t_R = 16.65 (linear gradient, 10–90% B, 30 min); MS (MALDI-TOF) m/z = 838.67 [M − 1].

Cyclic peptomer, PL-9.: Synthesis on 0.061 mmol scale. Purity of crude product 17.5% (C_{18} RP-HPLC). Yield after purification: 4 mg, 8%; white powder; RP-HPLC t_R = 21.08 (linear gradient, 0–70% B, 30 min); MS (MALDI-TOF) m/z = 826.62 $[M+H]^+$.

Cyclic peptomer, PL-10.: Synthesis on 0.062 mmol scale. Purity of crude product 53.6% (C_{18} RP-HPLC). Yield after purification: 13 mg, 25%; white powder; RP-HPLC t_R = 16.67 (linear gradient, 10–90% B, 30 min); MS (MALDI-TOF) m/z = 844.72 $[M+H]^+$.

Cyclic peptomer, PL-21.: Synthesis on 0.041 mmol scale. Purity of crude product 31% (C_{18} RP-HPLC). Yield after purification: 2.9 mg, 8%; white powder; RP-HPLC t_R = 12.88 (linear gradient, 10–90% B, 30 min); MS (MALDI-TOF) m/z = 870.18 $[M+H]^+$.

Cyclic peptomer, PL-22.: Synthesis on 0.036 mmol scale. Purity of crude product 14% (C_{18} RP-HPLC). Yield after purification: 1 mg, 3%; white powder; RP-HPLC t_R = 11.182 (linear gradient, 10–90% B, 30 min); MS (MALDI-TOF) m/z = 872.20 $[M+H]^+$.

Cyclic peptomer, PL-23.: Synthesis on 0.061 mmol scale. Purity of crude product 13% (C_{18} RP-HPLC). Yield after purification: 2.5 mg, 5%; white powder; RP-HPLC t_R = 12.48 (linear gradient, 10–90% B, 30 min); MS (MALDI-TOF) m/z = 877.31 [M − 1].

Cyclic peptomer, PL-28.: Synthesis on 0.061 mmol scale. Purity of crude product 7% (C_{18} RP-HPLC). Yield after purification: 3.3 mg, 6%; white powder; RP-HPLC t_R = 8.18 (linear gradient, 10–90% B, 30 min); MS (MALDI-TOF) m/z = 863.30 [M − 1].

Cyclic peptomer, PL-29.: Synthesis on 0.061 mmol scale. Purity of crude product 10% (C_{18} RP-HPLC). Yield after purification: 0.5 mg, 1%; white powder; RP-HPLC t_R = 10.20 (linear gradient, 10–90% B, 30 min); MS (MALDI-TOF) m/z = 766.30 $[M+H]^+$.

Cyclic peptomer, PL-30.: Synthesis on 0.061 mmol scale. Purity of crude product 13% (C_{18} RP-HPLC). Yield after purification: 4.7 mg, 9%; white powder; RP-HPLC t_R = 12.48 (linear gradient, 10–90% B, 30 min); MS (MALDI-TOF) m/z = 877.31 [M—1].

3.7. Synthesis of (*N*-[(9*H*-fluoren-9-yl)methoxycarbonyl]-*N*-(isobutyl)glycine) (11, Fmoc-*NLeu*-OH) from 1

3.7.1. Synthesis of ethyl 2-(isobutyl amino)acetate (H-*NLeu*-OEt)—Ethyl bromoacetate (50 mmol, 5.54 mL) in THF (25 mL) was added dropwise to a cooled (ice bath) solution of isobutylamine (110 mmol, 10.9 mL) in THF (25 mL). After stirring for 2.5 h at room temperature, the reaction mixture was concentrated in vacuo to remove THF and resuspended in ether. The mixture was filtered to remove isobutylaminehydrobromide, the residue washed with ether, and the filtrate concentrated in vacuo. Column chromatography (silica, eluent: ether) afforded H-*NLeu*-OEt (7.7 g, 48.4 mmol) as an oil in 97% yield (eluent: ether); ^{1}H NMR (300 MHz, $CDCl_3$): d 4.19 (q, J = 7.2 Hz, 2H), 3.39 (s, 2H), 2.41 (d, J = 6.7 Hz, 2H), 1.74 (quintet, 1H), 1.56 (br s, 1H), 1.28 (t, J = 7.2 Hz, 3H), 0.93 (d, J = 6.7 Hz, 6H).

3.7.2. *N*-[(9*H*-Fluoren-9-yl)methoxycarbonyl]-*N*-(isobutyl)glycine (11, Fmoc-*NLeu*-OH)—NaOH (4 N, 4.71 mL) was added to a solution of H-*NLeu*-OEt (18.84 mmol, 3 g) in dioxane (66 mL) and MeOH (24 mL). After stirring for 30 min at room temperature the reaction mixture was concentrated in vacuo to give H-*NLeu*-ONa.

The sodium salt was dissolved in water (18 mL) and the pH adjusted to 9–9.5 with 2 N HCl. Then, Fmoc-OSu (19.78 mmol, 1.05 equiv, 6.67 g) in 1,4-dioxane solution was added dropwise, and the reaction was continued with stirring at pH 8.5–9.0. After 1 h of stirring, the reaction was concentrated and worked up as follows: Excess Fmoc-OSu was washed out

with ether, and the aqueous phase was neutralized using 2 N HCl to pH 2–3. Ethyl acetate was used for extracting the resulting Fmocpeptoid. After back-washing with saturated NaCl and drying over Mg_2SO_4, evaporation of the solvent by a rotary evaporator gave the crude Fmoc-*NLeu*-OH as an oil. Crystallization (ether/hexanes) afforded Fmoc-*NLeu*-OH, 11(4 g, 11.3 mmol) as a white solid in 60% yield (eluent: DCM/ MeOH/HOAc, 90/10/0.5, v/v).

Fmoc-NLeu-OH, ***11***: The NMR spectra clearly show the presence of both rotamers.

^{1}H NMR (300 MHz, $CDCl_3$): d 7.73 (t, 2H), 7.51–7.58 (4 lines, 2H), 7.23–7.41 (m, 4H), 4.46, 4.54 (two d, J = 6.0 Hz, 2H), 4.16–4.25 (m, 1H), 3.87, 3.99 (two s, 2H), 2.93, 3.13 (two d, J = 7.5 Hz, 2H), 1.61, 1.82 (two septets, 1H), 0.72, 0.87 (two doublets, J = 6.8 Hz 6H). All data were in agreement with the reported values.[18]

3.7.3. Thioether-bridged cyclic peptomers having double peptoid

Cyclic peptomer, PL-11.: Synthesis on 0.041 mmol scale. Purity of crude product 21.6% (C_{18} RP-HPLC). Yield after purification: 2.2 mg, 8%; white powder; RP-HPLC t_R = 12.39 (linear gradient, 0–70% B, 30 min); MS (MALDI-TOF) m/z = 679.57 $[M+H]^+$.

Cyclic peptomer, PL-12.: Synthesis on 0.061 mmol scale. Purity of crude product 29.22% (C_{18} RP-HPLC). Yield after purification: 3.2 mg, 8%; white powder; RP-HPLC t_R = 11.59 (linear gradient, 0–70% B, 30 min); MS (MALDI-TOF) m/z = 679.56 $[M+H]^+$.

Cyclic peptomer, PL-13.: Synthesis on 0.041 mmol scale. Purity of crude product 30% (C_{18} RP-HPLC). Yield after purification: 3.2 mg, 9%; white powder; RP-HPLC t_R = 13.72 (linear gradient, 10–90% B, 30 min); MS (MALDI-TOF) m/z = 838.30 [M − 1].

Cyclic peptomer, PL-15.: Synthesis on 0.031 mmol scale. Purity of crude product 12% (C_{18} RP-HPLC). Yield after purification: 1.5 mg, 6%; white powder; RP-HPLC t_R = 13.80 (linear gradient, 10–90% B, 30 min); MS (MALDI-TOF) m/z = 877.31 [M − 1].

Cyclic peptomer, PL-16.: Synthesis on 0.031 mmol scale. Purity of crude product 26% (C_{18} RP-HPLC). Yield after purification: 3.6 mg, 14%; white powder; RP-HPLC t_R = 13.84 (linear gradient, 10–90% B, 30 min); MS (MALDI-TOF) m/z = 844.72 $[M+H]^+$.

Cyclic peptomer, PL-18.: Synthesis on 0.033 mmol scale. Purity of crude product 31% (C_{18} RP-HPLC). Yield after purification: 4.9 mg, 17%; white powder; RP-HPLC t_R = 12.56 (linear gradient, 10–90% B, 30 min); MS (MALDI-TOF) m/z = 870.18 $[M+H]^+$.

Cyclic peptomer, PL-19.: Synthesis on 0.031 mmol scale. Purity of crude product 26% (C_{18} RP-HPLC). Yield after purification: 0.8 mg, 3%; white powder; RP-HPLC t_R = 16.13 (linear gradient, 10–90% B, 30 min); MS (MALDI-TOF) m/z = 868.51 $[M+H]^+$.

Cyclic peptomer, PL-20.: Synthesis on 0.025 mmol scale. Purity of crude product 11% (C_{18} RP-HPLC). Yield after purification: 0.6 mg, 3%; white powder; RP-HPLC t_R = 13.93 (linear gradient, 10–90% B, 30 min); MS (MALDI-TOF) m/z = 838.67 [M—1].

3.8. Peptide synthesis using click chemistry

Macrocyclization using ring-closing [1,3] dipolar cycloaddition was undertaken using the protected monomeric sequences as described below. Chloro-trityl resin (0.061 mmol) was used to synthesize the fully side-chain-protected linear peptides which in turn cleaved from the resin under mild acidic conditions (TFA, DCM) affording compounds soluble in organic solvents.

The alkyne group was usually incorporated as an *N*-propargyl-glycine unit. The symmetric anhydride of 2-bromoacetic acid (5 equiv of anhydride relative to free amine) was prepared by mixing the acid (10 equiv) with *N*,*N*′ -diisopropylcarbodiimide (DIC, 5.0 equiv) in DMF at room temperature for 15 min. This mixture was then added to the resin and allowed to react for 3 h with stirring. The resin was washed and then treated with propargylamine (20.0 equiv) in DMF for 12–16 h. After washing, coupling of the next residue to the resultant secondary amine was achieved by usual procedure using HBTU, HOBt and DIEA for 1 h with stirring. Azide was incorporated by the attachment of 5-azidopropanoic acid by the standard peptide coupling procedure.

Click chemistry proceeded smoothly in the presence of CuI and 2,6-lutidine and at room temperature for 16 h. Removal of the side-chain protecting groups under acidic conditions followed by purification by preparatory HPLC to give a white powder.

3.9. Synthesis of 3-azidopropanoic acid (50)

3.9.1. Synthesis of 3-azidopropanoate—Methyl 3-bromopropanoate (1.09 mL, 10 mmol) and sodium azide (0.91 g, 14 mmol) were dissolved in DMSO (4.6 mL) in a 25 mL round bottom flask. The mixture solution was heated to 45 °C and stirred for 24 h. After the mixture was cooled down to room temperature, and extracted with diethyl ether. The combined organic layer was dried over anhydrous magnesium sulfate, filtered, and concentrated on a rotary evaporator to give azidopropanoate as colorless liquid (1.29 g, quan).

^{l}H NMR (300 MHz, $CDCl_3$) δ 3.62 (s, 3H), 3.47 (t, J = 6.3 Hz, 2H), 2.87 (t, J = 6.6 Hz, 2H).

3.9.2. 3-Azidopropanoic acid (50)—In a 50 mL flash, methyl 3-azidopropanoate (0.640 g, 4.96 mmol) was dissolved in 2 N NaOH (4.95 mL) solution. A small amount of MeOH was added slowly to make it homogeneous solution. The mixture was stirred at room temperature for 48 h, and then MeOH was removed under vacuo. The aqueous layer was washed with Et_2O, and then acidified with conc. HCl to pH 1. The compound was extracted with diethyl ether, and the combined organic fractions were dried over anhydrous magnesium sulfate, filtered, and concentrated on a rotary evaporator to give 50 as brownish liquid.

^{l}H NMR (300 MHz, $CDCl_3$) δ 11.55 (s, 1H), 3.57 (t, J = 6.6 Hz, 2H), 2.63 (t, J = 6.6 Hz, 2H). All data were in agreement with the reported values.[19]

Cyclic peptide 50.: Synthesis on 0.061 mmol scale. Purity of crude product 7% (C_{18} RP-HPLC). Yield after purification: 1.5 mg, 3%; RP-HPLC t_R = 12.82 min; (linear gradient, 10–90% B, 30 min) MS (MAL-DI-TOF) m/z 838.97 [M—3].

3.10. General synthetic procedure for the Indole analogues (24–116)

3.10.1. Synthesis of 1-amino-5-(1*H*-indol-3-yl)-pentan-3-one (24)—A solution of *N,N′* -dicyclohexylcarbodiimide (DCC, 2.06 g, 10 mmol) and Boc-β-Ala-OH (0.993 g, 5.25 mmol) was stirred in DCM (12 mL) for 10 min. Tryptamine (0.801 g, 5 mmol) was then added to the flask and the resulting mixture was stirred at room temperature overnight. The suspension was evaporated and filtered off using ethyl acetate. The resulting solution was washed with water and extracted with ethyl acetate. The combined organic layers were combined and dried with anhydrous magnesium sulfate, filtered and concentrated by rotary evaporation to give brown oil, 1.5 g, 4.67 mmol, 89%. The Boc group was then quantitatively removed by treatment with 8 mL of 1:1 trifluoroaceticacid: CH_2Cl_2 for 1 h at rt. The final compound, **24** was obtained by removal of solvents in vacuo.

3.10.1.1. tert-Butyl-5-(1H-indol-3-yl)-3-oxopentylcarbamate (24A).: ^{1}H NMR (300 MHz, $CDCl_3$) δ 8.82 (s, 1H), 7.57 (d, J = 7.80 Hz, 1H), 7.35 (d, J = 8.10 Hz, 1H), 7.18 (t, J = 8.80 Hz, 1H), 7.10 (t, J = 6.90 Hz, 1H), 6.97 (s, 1H), 6.07 (s,1H), 5.22 (s, 1H), 3.55 (q, J = 6.60 Hz, 2H), 3.35 (s, 2H), 2.94 (t, J = 6.60 Hz, 2H), 2.26 (t, J= 6.30 Hz, 2H), 1.46 (s, 9H).

3.10.1.2. 1-Amino-5-(1H-indol-3-yl)-pentan-3-one (24).: ^{1}H NMR (300 MHz, $CDCl_3$) δ 7.21 (d, J = 7.62 Hz, 1H), 6.99 (d, J = 7.95 Hz, 1H), 6.77–6.64 (m, 2H), 6.72 (s, 1H), 3.16 (t, J = 7.20 Hz, 2H), 2.78 (t, J = 6.33 Hz, 2H), 2.61(t, J = 7.14 Hz, 2H), 2.2 (t, J = 6.42 Hz, 2H).

Cyclic peptomer, PL-24.: Synthesis on 0.061 mmol scale. Purity of crude product 10% (C_{18}RP-HPLC). Yield after purification: 1.3 mg, 2.2%; white powder; RP-HPLC t_R = 17.85 (linear gradient, 10–90% B, 30 min); MS (MALDI-TOF) m/z = 953.40 [M+3].

3.11. Synthesis of 1-(1-acetyl-1*H*-indol-3-yl)-5-aminopentan-3-one (113)

tert-Butyl-5-(1*H*-indol-3-yl)-3-oxopentylcarbamate, **24A** (0.309 g, 0.93 mmol) and DMAP (0.022 g, 0.18 mmol) were taken in a round bottom flask fitted with reflux condenser under argon atmosphere. DMF (2.2 mL) was added to the flask via syringe followed by triethylamine (195 μL, 1.40 mmol), and acetic anhydride (168 μL, 1.77 mmol). The reaction was heated at 80 °C for 24 h. Upon cooling to room temperature the reaction was diluted with ethyl acetate and washed with a saturated solution of ammonium chloride, and the aqueous layer was further extracted with ethyl acetate. The combined organic layers were dried over magnesium sulfate and the solvent evaporated. The brown residue was purified by flash chromatography on silica gel with ethyl acetate/hexanes as the solvent to give pale yellow solid, 0.240 g, 0.643 mmol, 69%. The Boc group was then quantitatively removed by treatment with 1 mL of 1:1 trifluoroaceticacid/CH_2Cl_2 for 1 h at rt. The final compound, **113** was obtained by removal of solvents in vacuo.

3.11.1. *tert*-Butyl-5-(1*H*-indol-3-yl)-3-oxopentylcarbamate (113B)—^{1}H NMR (300 MHz, $CDCl_3$) δ 8.40 (d, J = 7.74 Hz, 1H), 7.53 (d, J = 7.26 Hz, 1H), 7.35–7.38 (m,1H),

7.33–7.30 (m, 1H), 7.26 (s, 1H), 6.19 (s, 1H), 5.21 (s, 1H), 3.60 (q, J = 6.84 Hz, 2H), 3.38 (q, J = 6.24 Hz, 2H), 2.91 (t, J = 7.02 Hz, 2H), 2.55 (s, 3H) 2.36 (t, J = 6.0 Hz, 2H), 1.41 (s, 9H).

3.11.2. 1-(1-Acetyl-1*H*-indol-3-yl)-5-aminopentan-3-one (113)—^{1}H NMR (300 MHz, $CDCl_3$) δ 8.27–8.24 (m, 1H), 7.52–7.49 (m, 1H), 7.40 (s, 1H), 7.25–7.16 (m, 2H), 3.46 (t, J = 7.20 Hz, 2H), 3.09 (t, J = 6.51 Hz, 2H), 2.84 (t, J = 7.17 Hz, 2H), 2.52 (t, J = 6.53 Hz, 2H), 2.51 (s, 3H).

Cyclic peptomer, PL-113.: Synthesis on 0.041 mmol scale. Purity of crude product 20% (C_{18} RP-HPLC). Yield after purification: 5 mg, 12%; white powder; RP-HPLC t_R = 14.95 (solvent gradient, 10–90% B, 30 min); MS (MALDI-TOF) m/z = 992.38 $[M+H]^+$.

3.12. Synthesis of 1-(1-acetyl-1*H*-indol-3-yl)-7-aminoheptan-3-one (119)

3.12.1. Synthesis of *tert*-butyl-7-(1*H*-indol-3-yl)-5-oxoheptylcarbamate (119A)—The title compound is synthesized in a manner identical to compound **24A**, absent of Boc-β-Ala-OH; instead Boc-5-Ava-OH (1.14 g, 5.25 mmol). Materials: Tryptamine (0.801 g, 5 mmol), and DCC (2.06 g, 10 mmol) in 13 mL DCM. The compound is purified by column chromatography on silica gel, eluted with 4% EtOAc–Hexane. Yield: Product **119A** (1.7 g, 4.95 mmol, 99%).

^{1}H NMR (300 MHz, $CDCl_3$) δ 8.29 (s, 1H), 7.61 (d, J = 7.80 Hz, 1H), 7.39 (d, J = 8.04 Hz, 1H), 7.24–7.19 (m, 1H), 7.16–7.10 (m, 1H), 7.04 (d, J = 2.28 Hz, 1H), 5.59 (s, 1H), 4.59 (s, 1H), 3.61 (q, J = 6.06 Hz, 2H), 3.08 (q, J = 6.36 Hz, 2H), 2.99 (t, J = 6.69 Hz, 2H), 2.12 (t, J = 7.32 Hz, 2H), 1.59 (q, J = 7.98 Hz, 2H), 1.48–1.41 (m, 2H) 1.43 (s, 9H).

3.13. 1-(1-Acetyl-1*H*-indol-3-yl)-7-aminoheptan-3-one (119)

The title compound is synthesized in a manner identical to compound **113**, absent of **24A**; instead **119 A** (1.11 g, 3.23 mmol). Materials: DMAP (0.075 g, 0.62 mmol), triethylamine (675 μL, 4.85 mmol), and acetic anhydride (580 μL, 6.14 mmol) in 7.5 mL DMF. The compound is purified by column chromatography on silica gel, eluted with 2% EtOAc–Hexane. Yield: Product **119B** (0.905 g, 2.25 mmol, 70%). The Boc group was then quantitatively removed by treatment with 3.6 mL of 1:1 trifluoroaceticacid/CH_2Cl_2 for 1 h at rt. The final compound, **119** was obtained by removal of solvents in vacuo.

3.13.1. *tert*-Butyl-7-(1-acetyl-1*H*-indol-3-yl)-5-oxoheptylcarbamate (119B)—^{1}H NMR (300 MHz, $CDCl_3$) 03b3δ 8.43 (d, J = 8.16 Hz, 1H), 7.56 (d, J = 7.11 Hz, 1H), 7.42–7.29 (m, 3H), 7.27 (s, 1H), 5.77 (s, 1H), 4.60 (s, 1H), 3.62 (q, J = 6.62 Hz, 2H), 3.11 (q, J = 6.45 Hz, 2H), 2.93 (t, J = 6.86 Hz, 2H), 2.62 (s, 3H) 2.18 (t, J = 7.40 Hz, 2H), 1.71–1.59 (m, 2H), 1.44–1.54 (m, 2H), 1.43 (s, 9H).

3.13.2. 1-(1-Acetyl-1*H*-indol-3-yl)-7-aminoheptan-3-one (119)—^{1}H NMR (300 MHz, $CDCl_3$) δ 7.61–7.38 (m, 1H), 7.37–7.13 (m, 1H), 7.12–6.85 (m, 3H), 3.43–3.28 (m, 2H), 3.06–2.90 (m, 2H), .88–2.61 (m, 4H), 2.18–2.04 (m, 2H), 2.57 (s, 3H), 1.35–1.21 (m, 2H).

Cyclic peptomer, PL-119.: Synthesis on 0.041 mmol scale. Purity of crude product 23% (C_{18} RP-HPLC). Yield after purification: 4.8 mg, 11%; white powder; RP-HPLC t_R = 18.01 (solvent gradient, 10–90% B, 30 min); MS (MALDI-TOF) m/z = 1020.41 $[M+H]^+$.

3.14. Synthesis of 1-(1-acetyl-1*H*-indol-3-yl)-8-aminooctan-3-one (116)

3.14.1. Synthesis of *tert*-butyl-8-(1*H*-indol-3-yl)-6-oxooctylcarbamate (116A)—

The title compound is synthesized in a manner identical to compound **24A**, absent of Boc-β-Ala-OH; instead Boc-6-Ahx-OH (1.5 g, 6.49 mmol). Materials: Tryptamine (0.990 g, 6.17 mmol), and DCC (2.55 g, 12.34 mmol) in 40 mL DCM. The compound is purified by column chromatography on silica gel, eluted with 3% EtOAc–Hexane. Yield: Product 116A (2.2 g, 5.90 mmol, 90%).

^{1}H NMR (300 MHz, $CDCl_3$) δ 9.27 (s, 1H), 7.57 (d, J = 7.74 Hz, 1H), 7.35 (d, J = 8.07 Hz, 1H), 7.17 (t, J = 7.05 Hz, 1H), 7.08 (t, J = 7.86 Hz, 1H), 6.97 (d, J = 1.90 Hz, 1H) 5.98 (t, J = 5.44 Hz, 1H), 4.84 (s, 1H), 3.56 (q, J = 6.37 Hz, 2H), 3.10–2.99 (m, 2H), 2.95 (t, J = 6.78 Hz, 2H), 2.09–2.0 (m, 2H), 1.47 (s, 9H), 1.44–1.32 (m, 2H),1.27–1.17 (m, 2H).

^{13}C NMR (75 MHz, $CDCl_3$) δ 172.9, 156.2, 136.6, 127.3, 122.4, 122.0, 119.2, 118.6, 112.5, 111.4, 79.2, 40.4, 39.6, 36.5, 29.8, 28.4, 26.3, 25.3, 25.2.

3.14.2. Synthesis of 1-(1-acetyl-1*H*-indol-3-yl)-8-aminooctan-3-one (116)—

The title compound is synthesized in a manner identical to compound **113**, absent of **24A**; instead **116A** (0.754 g, 2.02 mmol). Materials: DMAP (0.047 g, 0.386 mmol), triethylamine (423 μL, 3.03 mmol), and acetic anhydride (363 μL, 3.84 mmol) in4.6 mL DMF. The compound is purified by column chromatography on silica gel, eluted with 2% EtOAc–Hexane. Yield: Product **116B** (0.637 g, 1.53 mmol, 76%). The Boc group was then quantitatively removed by treatment with 2.6 mL of 1:1 trifluoroaceticacid/CH_2Cl_2 for 1 h at rt. The final compound, **116** was obtained by removal of solvents in vacuo.

3.14.2.1. *tert*-Butyl-8-(1-acetyl-1H-indol-3-yl)-6-oxooctylcarbamate (116B).: ^{1}H NMR (300 MHz, $CDCl_3$) δ 8.39 (d, J = 7.92 Hz, 1H), 7.54 (d, J = 7.32 Hz, 1H), 7.40–7.24 (m, 3H), 6.12 (s, 1H), 4.68 (s, 1H), 3.60 (q, J = 6.84 Hz, 2H), 3.06 (q, J = 6.36 Hz, 2H), 2.55 (s, 3H), 2.14 (t, J = 7.32 Hz, 2H), 1.69–1.54 (m, 2H), 1.51–1.44 (m, 2H), 1.42 (s, 9H), 1.36–1.23 (m, 4H).

^{13}C NMR (75 MHz, $CDCl_3$) δ 173.2, 168.5, 156.1, 135.9, 130.5, 125.3, 123.6, 122.6, 119.8, 118.8, 116.6, 79.1, 40.3, 38.9, 36.5, 29.7, 28.4, 26.3, 25.3, 25.2, 23.9.

3.14.2.2. 1-(1-Acetyl-1H-indol-3-yl)-8-aminooctan-3-one (116).: ^{1}H NMR (300 MHz, $CDCl_3$) δ 8.40 (d, J = 7.32 Hz, 1H), 7.69–7.63 (m, 1H), 7.58 (s, 1H), 7.41–7.29 (m, 2H), 3.59 (t, J = 7.07 Hz, 2H), 2.98 (t, J = 7.04 Hz, 2H), 2.90 (t, J = 7.5 Hz, 2H), 2.68 (s, 3H), 2.23 (t, J = 7.31 Hz, 2H), 1.72–1.57 (m, 4H), 1.42– 1.32 (m, 2H).

Cyclic peptomer, PL-116.: Synthesis on 0.041 mmol scale. Purity of crude product 29% (C_{18} RP-HPLC). Yield after purification: 6.5 mg, 15%; white powder; RP-HPLC t_R = 15.55 (solvent gradient, 10–90% B, 30 min); MS (MALDI-TOF) m/z = 1034.49 $[M+H]^+$.

3.15. Synthesis of *N*(*α*)-[(9*H*-fluoren-9-ylmethoxy)carbonyl-[*N*(*π*)-(8-phenyl octyl)]-$_L$-histidine (120)

3.15.1. Synthesis of *N*(*α*)-[(9*H*-fluoren-9-ylmethoxy)carbonyl-[*N*(*τ*)-(trityl)]-$_L$-histidine methyl ester (C)—

A 100 mL Schlenk flask is charged with solid Fmoc-His(Trt)-OH (10 g, 16.14 mmol), HOBt (3.27 g, 24.2 mmol) and degassed by vacuum-Ar purge cycle. Dry THF (81 mL) is added to dissolve all solids and the solution is cooled to 13 °C with an ice-acetone bath. To this mixture, a dry THF solution (81 mL) of DCC (3.33 g, 16.14 mmol) is added along with 12.4 mL of MeOH dropwise over 30 min. The reaction is allowed to warm slowly to room temperature while stirring overnight (16 h), during which time solid dicyclohexylurea is observed to precipitate. This is removed by vacuum filtration through a medium-porosity frit and the solvent is removed by rotary evaporation. The oily residue is redissolved in dichloromethane, washed three times with saturated $NaHCO_3$ (aq), three times with water, and the organic layer is dried over Mg_2SO_4. The solvent is removed by rotary evaporation and a crude yellow solid is isolated after drying. The compound is purified by column chromatography on silica gel, eluted with 1% MeOH–DCM (Yield: 10.34 g, quan.). The compound is purified by column chromatography on silica gel, eluted with 1% MeOH/DCM. (Yield: 6.89 g, 83.6%).

^{1}H NMR (300 MHz, $CDCl_3$) δ 7.75 (d, J = 7.5 Hz, 2H), 7.62 (t, J = 7.0 Hz, 2H), 7.42–7.24 (m, 17H), 7.14–7.09 (m, 7H), 6.57 (s, 1H), 6.51 (d, J = 8.2 Hz, 1H), 4.38–4.22 (m, 2H), 4.12 (m, 1H), 3.63 (s, 3H), 3.06 (m, 2H).

3.15.2. Synthesis of *N*(*α*)-[(9*H*-fluoren-9-ylmethoxy) carbonyl-[*N*(*π*)-(8-phenyloctyl)-$_L$-histidinemethylester (D)—

To a stirred solution of triflic anhydride (0.443 mL, 2.63 mmol) in DCM (17 mL) under Ar at 75 °C was added a solution of 8-phenyl-1-octanol (0.578 mL, 2.63 mmol) and diisopropylethylamine (DIEA) (0.459 mL, 2.63 mmol) in DCM (12 mL) dropwise over 10 min. Stirring was continued at 75 °C (20 min), then a solution of Fmoc-His(Trt)-OMe (1.5 g, 2.37 mmol) in DCM (20 mL) was added dropwise, and the mixture was allowed to gradually warm to room temperature over a period of 16 h. The mixture was quenched using aqueous $NaHCO_3$ and stirred vigorously (30 min). The organic layer was diluted with DCM and washed with aqueous $NaHCO_3$ and brine, then dried (Mg_2SO_4), and concentrated to viscous oil. To a solution of the resulting gum in DCM (13 mL) was added trifluoroacetic acid (1.77 mL, 23.7 mmol) and triisopropylsilane (TIS) (0.534 mL, 2.61 mmol), and the mixture was stirred at room temperature until reaction was complete as shown by TLC (2 h). The solvent was removed in vacuo, and the residue was purified by silica gel column chromatography using 1–5% MeOH in DCM provided product as colorless gum (1.45 g, quan).

^{1}H NMR (300 MHz, $CDCl_3$) δ 8.37 (s, 1H), 7.77 (d, J = 7.41 Hz, 2H), 7.58 (m, J = 7.47 Hz, 1H), 7.38 (t, J = 7.14 Hz, 2H), 7.36–7.22 (m, 4H), 7.21–7.13 (m, 4H), 5.77–5.67 (m, 1H), 4.62–4.50 (m, 1H), 4.48–4.37 (m, 2H), 4.20 (t, J = 6.49 Hz, 1H), 4.04–3.93 (m, 2H) 3.78 (s, 3H), 3.27–3.13 (m, 2H), 2.58 (t, J = 7.77 Hz, 2H), 1.85–1.71 (m, 2H), 1.67–1.49 (m, 2H) 1.29 (s, 8H). MS (MALDI-TOF) m/z 580.17 $[M+H]^+$.

3.15.3. *N(α)*-[(9*H*-Fluoren-9-ylmethoxy) carbonyl-[*N*(π)-(8-phenyloctyl)-$_L$-histidine (120)—1:1 Mixture of 2 N HCl (48 mL) and 1,4-dioxane (48 mL) solution were added to the **D** (1.45 g, 2.5 mmol) and reflux at 100 °C for 3 h. The mixture was brought to room temperature, and the solvent was removed by Rota vapor. The resulting aqueous mixture was extracted with DCM, washed with brine, dried (Mg_2SO_4), concentrated to viscous oil, and then the residue was purified by silica gel flash chromatography from 5% to 20% MeOH in DCM to provide acid, **120** as a light yellow gum (0.903 g, 1.6 mmol, 64% yield.

^{l}H NMR (300 MHz, $CDCl_3$) δ 9.98 (br s, 1H), 8.37 (s, 1H), 7.74 (d, *J* = 7.41 Hz, 2H), 7.56 (t, *J* = 6.42 Hz, 2H), 7.37 (t, *J* = 7.32 Hz, 2H), 7.28 (t, *J* = 6.57 Hz, 3H), 7.17 (t, *J* = 8.12 Hz, 4H), 6.50 (br s, 1H), 4.61–4.47 (m, 1H), 4.35 (d, *J* = 6.15 Hz, 2H), 4.17 (t, *J* = 6.57 Hz, 1H), 4.08–3.85 (m, 2H), 3.35–3.17 (m, 2H), 2.56 (t, *J* = 7.47 Hz, 2H), 1.62–1.48 (m, 2H), 1.21 (s, 10H).

^{13}C NMR (75 MHz, $CDCl_3$) δ 172.4, 156.2, 144.2, 143.8, 142.9, 141.8, 134.2, 130.0, 128.8, 128.7, 128.2, 127.5, 126.1, 125.3, 120.4, 119.4, 66.8, 53.0, 47.1, 46.9,, 35.8, 31.3, 30.0, 29.1, 29.0, 28.8, 26.3, 25.8. MS (MALDI-TOF) *m*/*z* 566.37 $[M+H]^+$. All data were in agreement with the reported values.[21]

Cyclic peptomer, PL-120.: Synthesis on 0.040 mmol scale. Purity of crude product 16% (C_{18} RP-HPLC). Yield after purification: 1.1 mg, 2.2%; White powder; RP-HPLC t_R = 22.54 min (linear gradient, 5–95% B, 35 min); MS (MALDI-TOF) *m*/*z* 1222.63 $[M+H]^+$.

3.16. ELISA-based PBD-binding inhibition assay

A biotinylated p-T78 peptide was diluted with coating solution (KPL, Inc., Gaithersburg, MD) to the final concentration of 0.3 μM, and then 50 μL of the resulting solution was immobilized onto a 96-well streptavidin-coated plate (Nalgene Nunc, Rochester, NY). The wells were washed once with PBS + 0.05% Tween 20 (PBST) and incubated with 200 μL of PBS + 1% BSA (blocking buffer) for 1 h to prevent the unoccupied sites. Mitotic 293A lysates expressing HA-EGFP-Plk1 were prepared in TBSN buffer (60 μg total lysates in 100 μL) and applied onto the biotinylated peptide-coated ELISA wells immediately after mixing with the indicated amount of the competitor peptides, and then incubated with constant rocking for 1 h at 25 °C. Next, the plates were washed four times with PBST, and to detect the bound HA-EGFP-Plk1, the plates were incubated for 2 h with 100 μL/well of anti-HA antibody at a concentration of 0.5 μg/mL in the blocking buffer and then washed five times. Further, the plates were incubated with 100 μL/well of secondary antibody at a 1:1000 dilution in the blocking buffer. After-ward, the plates were washed five times with PBST and incubated with 100 μL/well of 3,3′,5,5′-tetramethylbenzidine (TMB) substrate solution (Sigma, St. Louis, MO) until a desired absorbance was achieved. The reactions were terminated by the addition of 1 N H_2SO_4, and the optical densities were measured at 450 nm using an ELISA plate reader (Molecular Device, Sunnyvale, CA). Data are shown in Figure. 2, 4 and 5; Supplementary Figure S2.

3.17. Fluorescence polarization assays

5-Carboxyfluorescein-labeled peptides (5-carboxyfluorescein-Ahx-DPPLHS-pT-AI-NH_2 for Plk1 PBD, 5-carboxyfluorescein-Ahx-GPMQTS-pT-PKNG for Plk2 PBD, and 5-carboxyfluorescein-Ahx-GPLATS-pT-PKNG for Plk3 PBD; final concentrations: 25 nM) were incubated with the bacterially-expressed purified PBDs of Plk1, Plk2 and Plk3 (final concentrations: 15 nM, 50 nM, and 500 nM, respectively) in a binding buffer containing 10 mM Tris (pH 8.0), 1 mM EDTA, 50 mM NaCl, and 0.01% Nonidet P-40. Indicated gradual concentration of compounds was provided into the reaction. Fluorescence polarization was analyzed 10 min after mixing of all components in the 384-well format using a Molecular Devices Spectra Max Paradigm Multi-Mode Microplate Detection Platform. All experiments were performed in triplicate

3.18. Molecular modeling methods

Theoretical calculations were performed using Discover 2.98/Insight II with CVFF force field as described previously.[22] The synthetic peptides such as PL-1, PL-5, PL-50, PL-116, and PL-120 were built from the coordinates of the pThr mimetic-containing PLHSpT as found in the crystal structure using the Builder module in In-sight II. The computational complex model was solvated using a solvent sphere of water extending 30.0 Å around the phosphate atom of pThr. The system was initially minimized using 1000 steps of steepest decent and 3000 steps of conjugated gradient with a 14.0 Å nonbonded cutoff distance. Data are shown in Figures 2 and 7; Supplementary Figure S1.

Supplementary Material

Refer to Web version on PubMed Central for supplementary material.

Acknowledgments

This work was supported in part by the Korea Basic Science Institute's research Grant T33418 (J. K. B.), the National Cancer Institute's Intramural Research Grant (K.S.L.), and the National Research Foundation of Korea (NRF)'s basic research program (2010–0019306) (D.Y.Y.).

References and notes

1. Ortutay C; Valiaho J; Stenberg K; Vihinen M. Hum. Mutat 2005, 25, 435. [PubMed: 15832311]
2. Bogoyevitch MA; Ban RK; Ketterman AJ Biochim. Biophys. Acta 2005, 1754, 79. [PubMed: 16182621]
3. Park J-E; Soung N-K; Johmura Y; Kang YH; Liao C; Lee KH; Park CH; Nicklaus MC; Lee KS Cell. Mol. Life Sci 2010, 67, 1957. [PubMed: 20148280]
4. Murugan RN; Park J-E; Kim E-H; Shin SY; Cheong C; Lee KS; Bang JK Mol. Cells 2011, 32, 209 and references therein. [PubMed: 21809214]
5. Kang YH; Park JE; Yu LR; Soung KK; Yun SM; Bang JK; Seong YS; Yu H; Garfield S; Veenstra TD; Lee KS Mol. Cell 2006, 24, 409. [PubMed: 17081991]
6. Yun S-M; Moulaei T; Lim D; Bang JK; Park J-E; Shenoy Shilpa R; Liu F; Kang YH; Liao C; Soung N-K; Lee S; Yoon D-Y; Lim Y; Lee D-H; Otaka A; Appella E; McMahon JB; Nicklaus MC; Burke TR Jr.; Yaffe MB; Wlodawer A; Lee KS Nat. Struct. Mol. Biol 2009, 16, 876. [PubMed: 19597481]
7. Liu F; Park J-E; Qian W-J; Lim D; Garber M; Berg T; Yaffe MB; Lee KS; Burke TR Jr. Nat. Chem. Biol 2011, 7, 595. [PubMed: 21765407]

8. Liu F; Park J-E; Qian W-J; Lim D; Scharow A; Berg T; Yaffe MB; Lee KS,; Burke TR Jr. ACS Chem. Biol 2012, 7, 805. [PubMed: 22292814]
9. Liu F; Park J-E; Qian W-J; Lim D; Scharow A; Berg T; Yaffe MB; Lee KS,; Burke TR Jr. Chembiochem 2012, 13, 1291. [PubMed: 22570300]
10. Qian WJ; Park JE; Lee KS; Burke TR Jr. Bioorg. Med. Chem. Lett 2012, 15, 7306.
11. Qian WJ; Park JE; Liu F; Lee KS; Burke TR Jr. Bioorg. Med. Chem in press.
12. Liao C; Park J-E; Bang JK; Nicklaus MC; Lee KS ACS Med. Chem. Lett 2010, 1, 110. [PubMed: 20625469]
13. Zuckermann RN; Kerr JM; Kent SBH; Moos WH J. Am. Chem. Soc 1992, 114, 10646.
14. Simon RJ; Kania RS; Zuckermann RN; Huebner VD; Jewell DA; Banville S; Ng S; Wang L; Rosenberg S; Marlowe CK; Spellmeyer DC; Tan R; Frankel AD; Santi DV; Cohen FR; Bartlett PA Proc. Natl. Acad. Sci. U.S.A 1992, 89, 9367. [PubMed: 1409642]
15. Yoo B; Shin SBY; Huang ML; Kirshenbaum K. Chem. Eur. J 2010, 16, 5528. [PubMed: 20414912]
16. Kim Y-K; Arai MA; Arai T; Lamenzo JO; Dean EF III; Patterson N; Clemons PA; Schreiber SL J. Am. Chem. Soc 2004, 126, 14740. [PubMed: 15535697]
17. Leung GC; Hudson JW; Kozarova A; Davidson A; Dennis JW; Sicheri F. Nat. Struct. Biol 2002, 10, 719.
18. Kruijtzer JAW; Liskamp RM J. Tetrahedron Lett 1995, 36, 6969.
19. Zhou Y; Wang S; Xie Y; Guan W; Ding B; Yang Z; Jiang X. Nanotechnology 2008, 19, 175601.
20. Wang X; Zhu J; Smithrud BD J. Org. Chem 2010, 75, 3358. [PubMed: 20411910]
21. Qian W; Liu F; Burke TR Jr. J. Org. Chem 2011, 76, 8885. [PubMed: 21950469]
22. Hagler AT; Lifson S; Dauber P. J. Am. Chem. Soc 1979, 101, 5122.

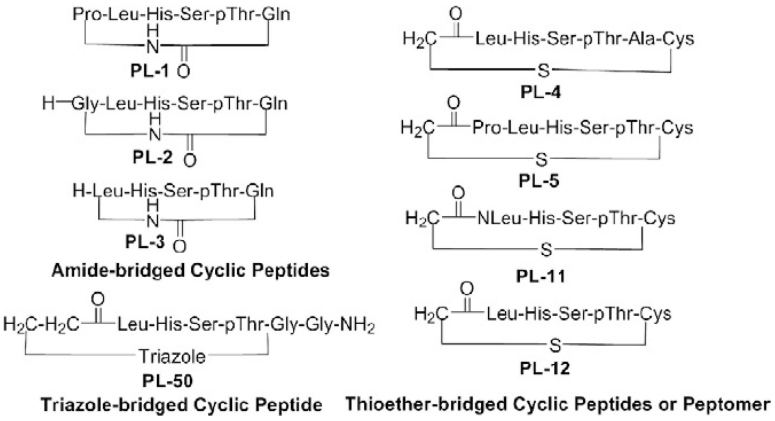

Figure 1.

First-phase cyclic peptide or peptomer derivatives (categories I–III) generated using solid-phase peptide synthesis (SPPS).

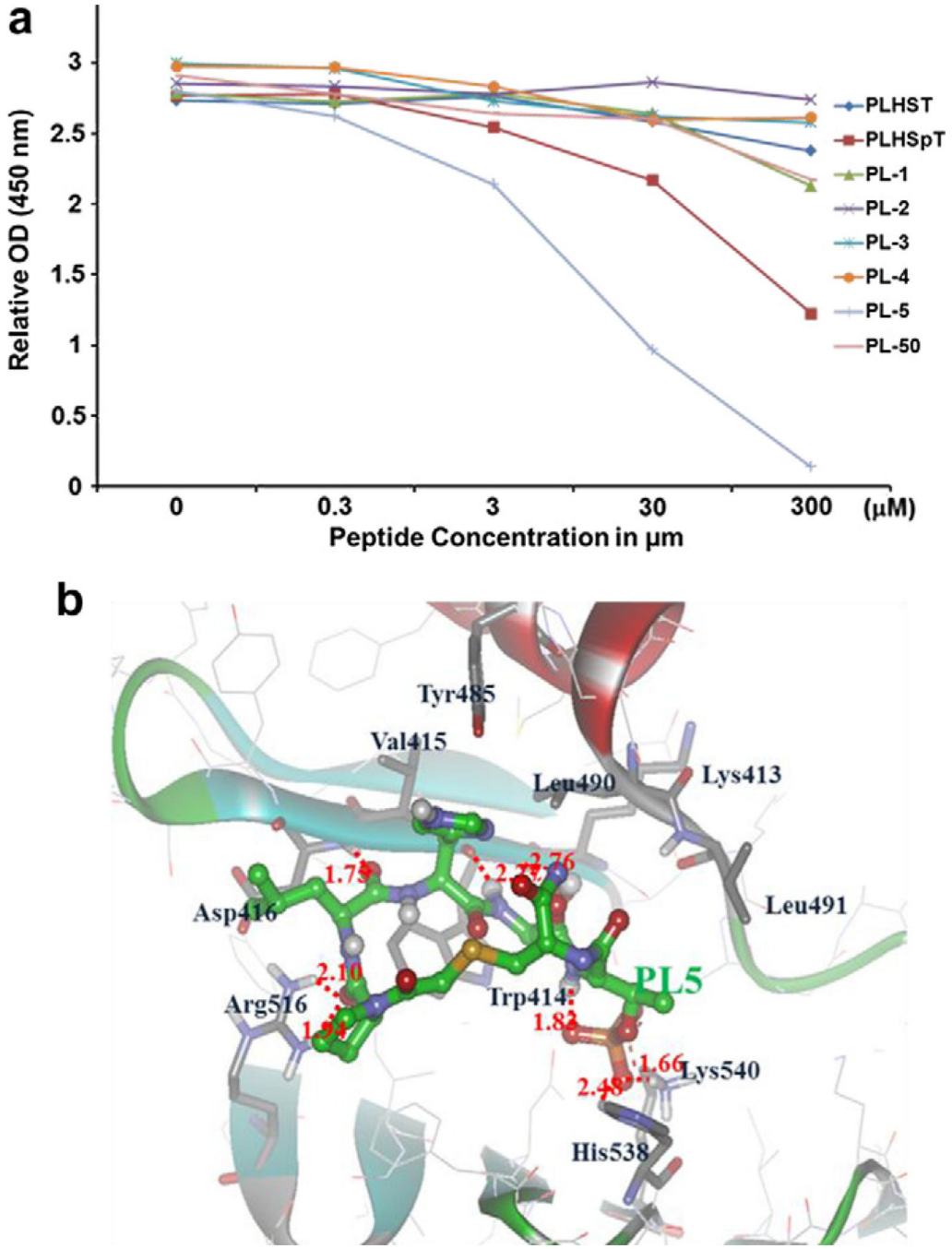

Figure 2.

Quantification and binding nature of cyclic peptomers. (a) An ELISA-based assay was used to determine the efficiency of Plk1 PBD inhibition by the indicated first-phase cyclic peptide or peptomer derivatives. Representative graphs are shown from three independent experiments. (b) PL-5 was docked into the ligand binding site and energy minimized with respect to pThr residue pointing toward the PBD of Plk1. This model predicts that the residues, such as pThr and Pro, contribute to the high binding affinity and specificity against Plk1 PBD.

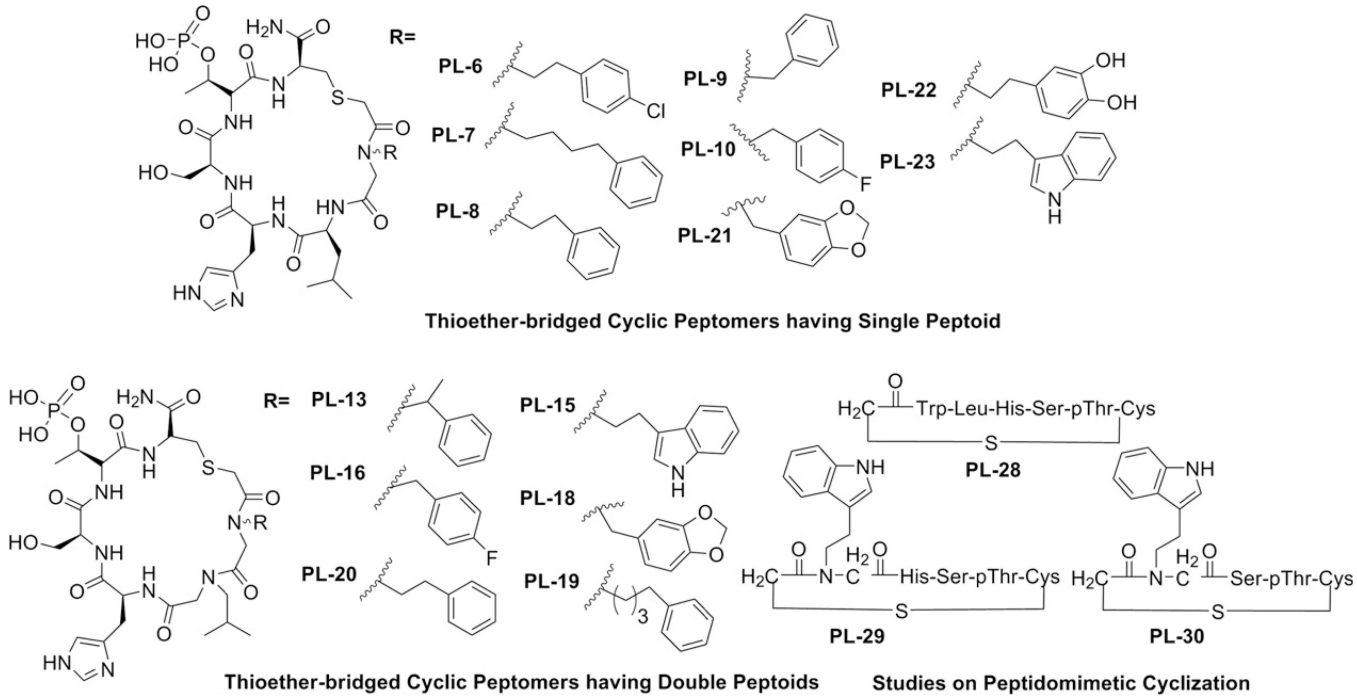

Figure 3.

First-phase cyclic peptomers (category IV) generated using solid-phase peptide synthesis (SPPS).

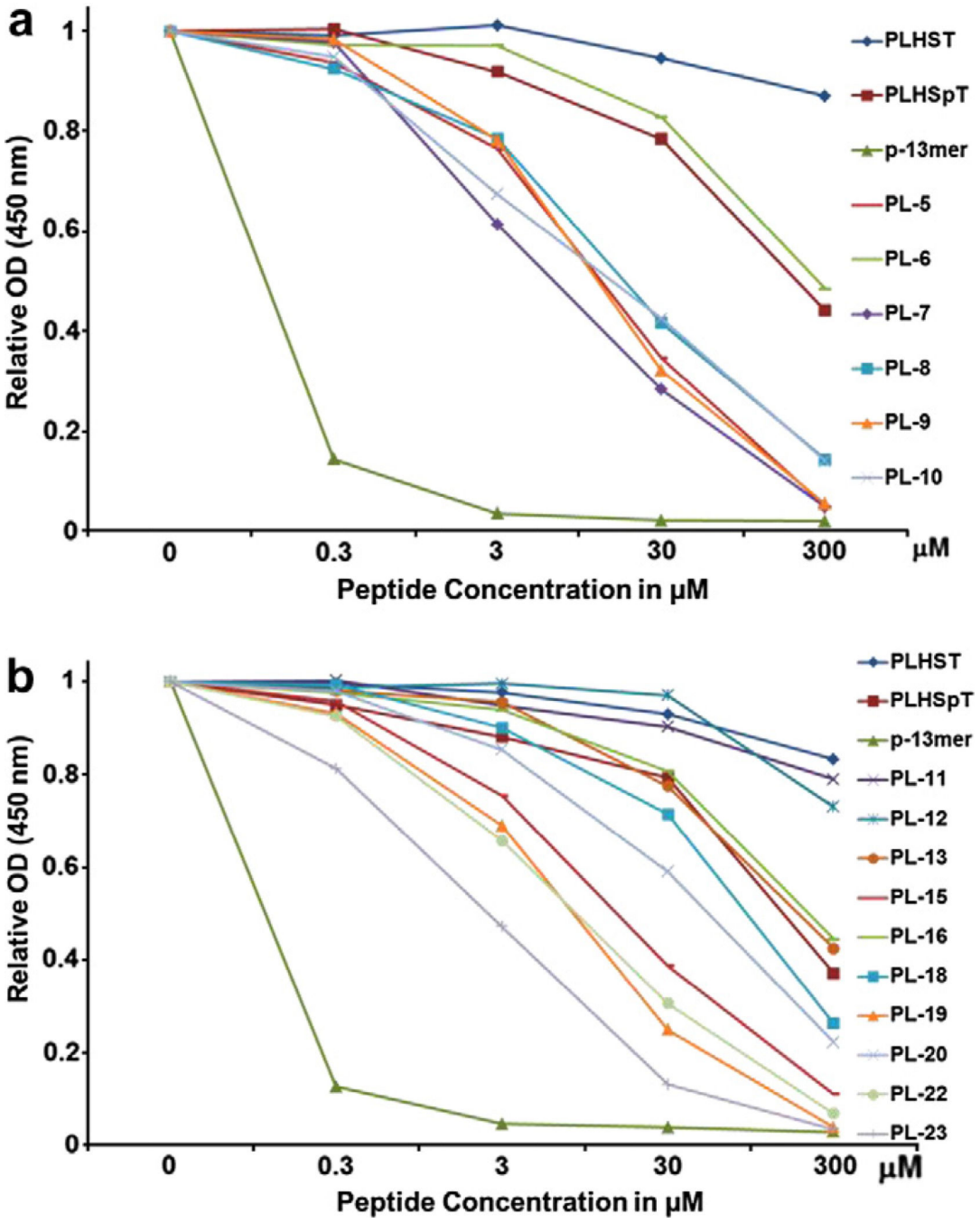

Figure 4.

An ELISA-based assay was used to determine the efficiency of Plk1 PBD inhibition by the indicated first-phase cyclic peptide or peptomer derivatives. Representative graphs are shown from three independent experiments. *p-13mer: Ac-ETFDPPLHSpTAIY-NH_2.

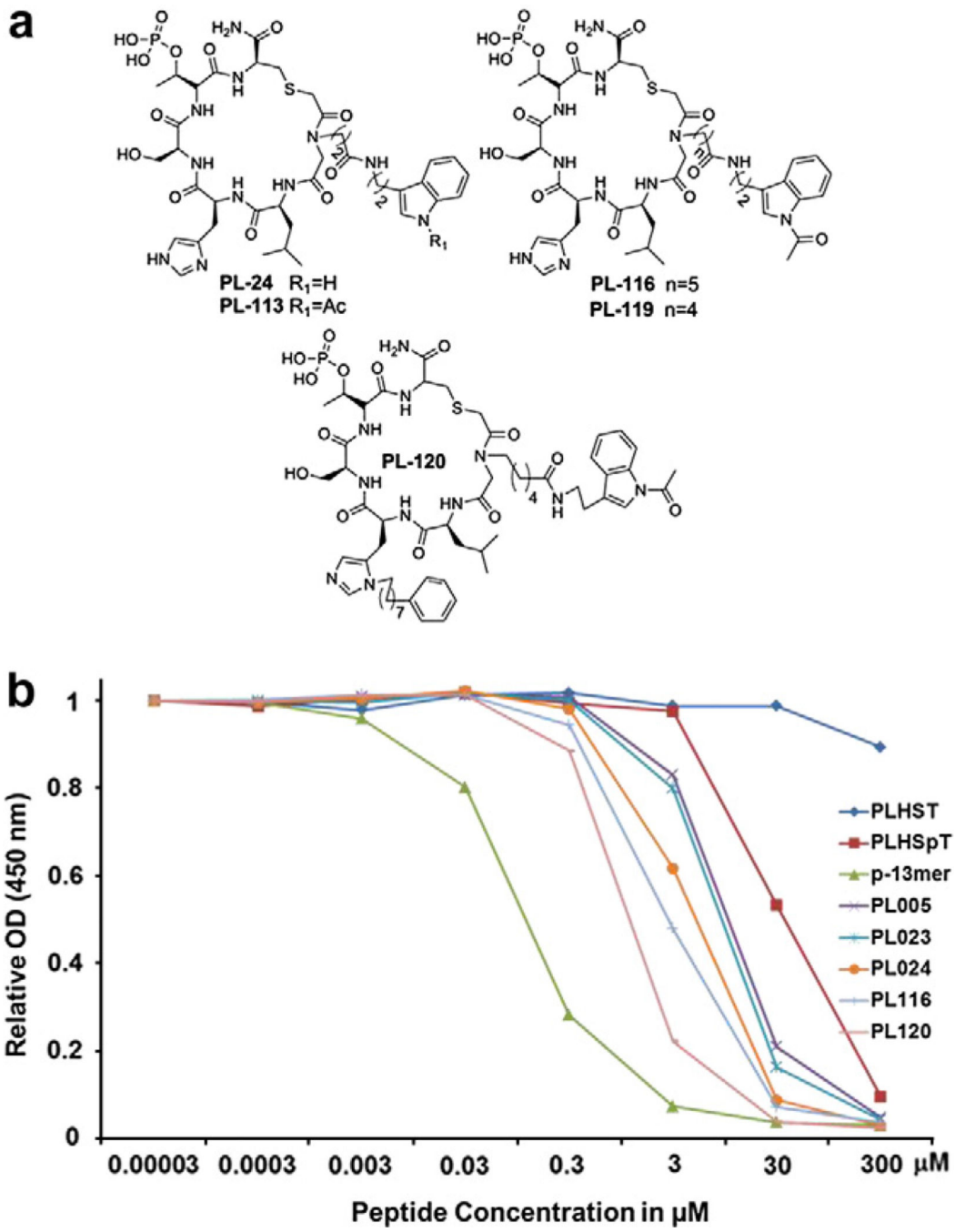

Figure 5.

Compounds generated from the second-phase diversification and quantification of their inhibitory activities against Plk1 PBD. (a) Chemical structures of second-phase cyclic peptomer derivatives. (b) ELISA-based Plk1 PBD-binding IC_{50} graph. O.D., optical density. A representative graph from three independent experiments is shown.*p-13mer: Ac-ETFDPPLHSpTAIY-NH_2.

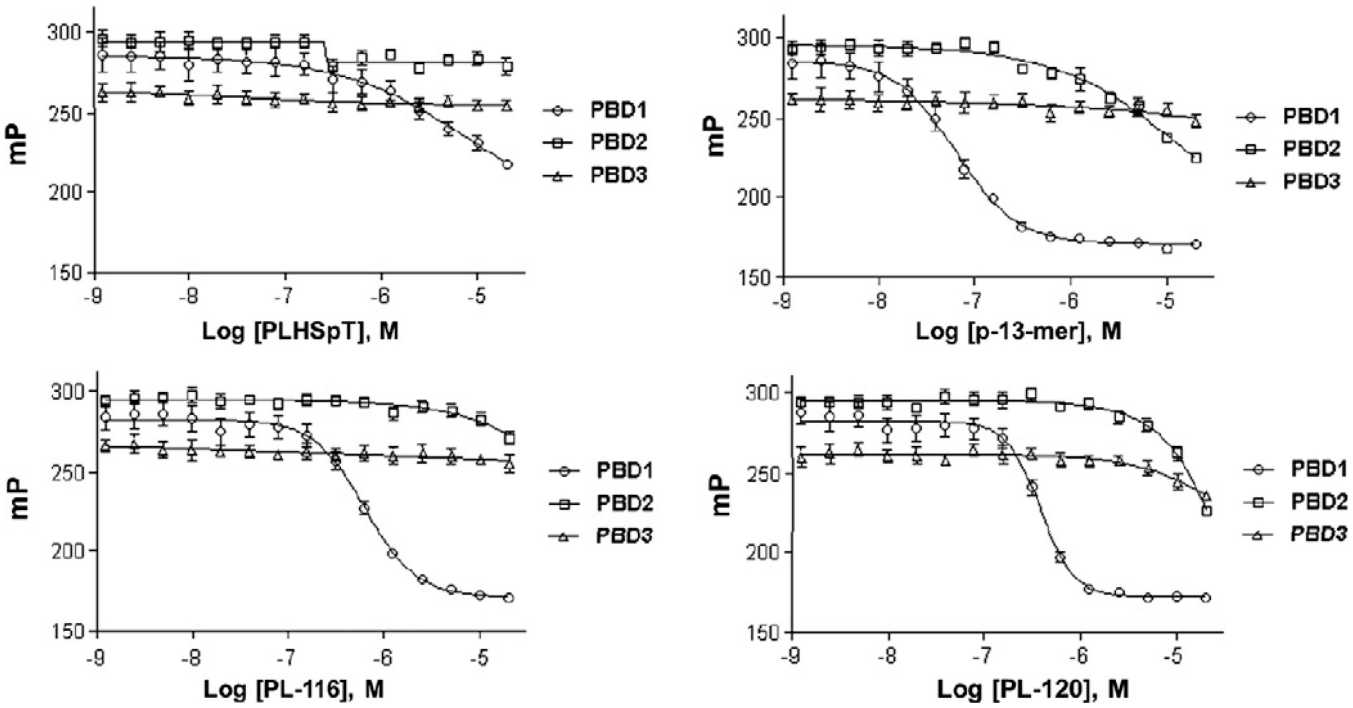

Figure 6.

Comparison of fluorescence polarization-based assays showing the selective inhibition of Plk1 PBD over Plk2 and 3 PBDs by PL-116 and PL-120.

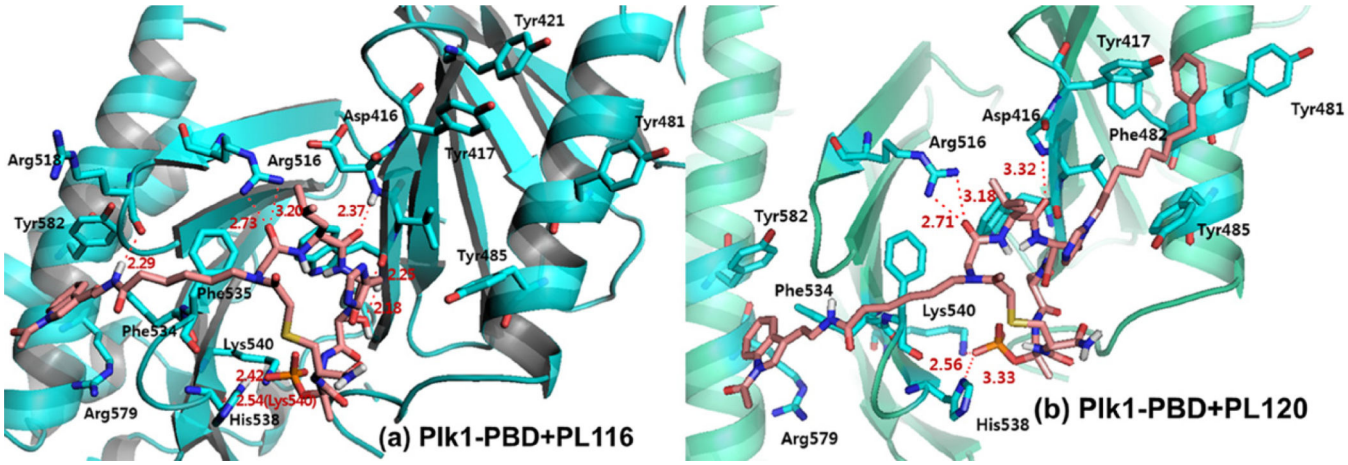

Figure 7.

The binding nature of cyclic peptomers. (a) A molecular model of PL-116 docked into the ligand binding site and energy-minimized with respect to the pThr residue pointing toward the PBD of Plk1. (b) A molecular modeling of Plk1-PBD in complex with PL-120. The modeling was done using Discover 2.98/Insight II with CVFF force field.

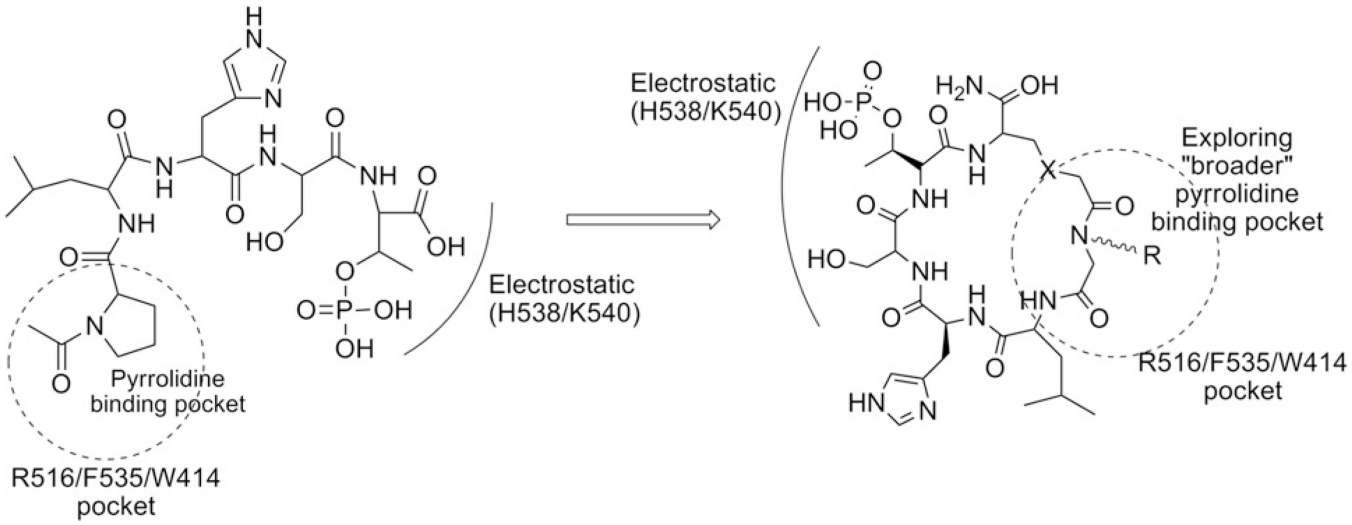

Scheme 1.

Binding nature of linear peptide, PLHSpT with Plk1 PBD, and illustration of the peptidomimetic cyclization.

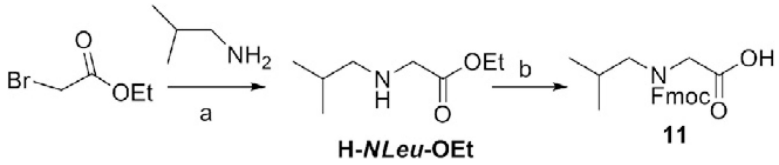

Scheme 2.

Reagents and conditions: (a) isobutylamine (2.2 equiv), THF, 0 °C, 2.5 h, 97%; (b) (1) 4 N NaOH, MeOH/1,4-dioxane (v/v, 1/4), rt, 0.5 h; (2) Fmoc-OSu, pH 8.5–9.0, 1,4-dioxane, rt, 1 h, 60% for two steps.

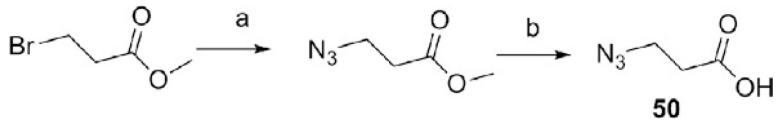

Scheme 3.

Reagents and conditions: (a) sodium azide (1.4 equiv), DMSO, 45 °C, 24 h, quan; (b) (1) 2 N NaOH, MeOH, rt, 48 h.

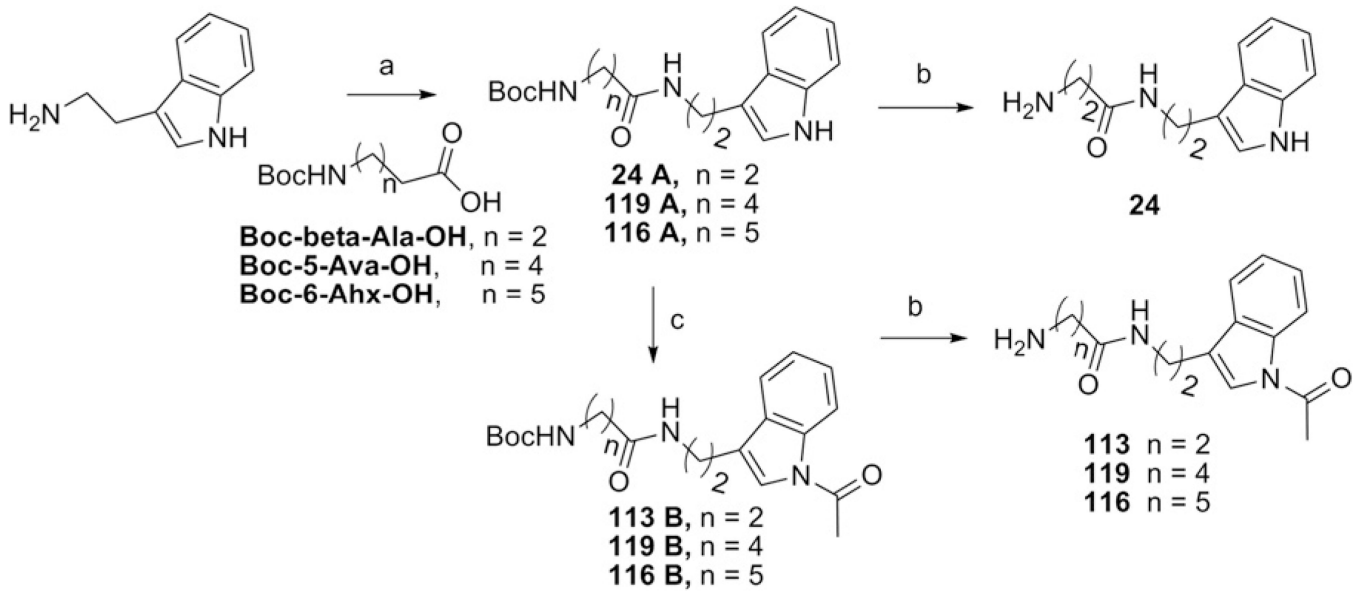

Scheme 4.

Reagents and conditions: (a) acid (1.05 equiv), DCC (2 equiv), DCM, rt, overnight, 90–99%; (b) TFA/CH_2Cl_2 (v/v, 1/1), rt, 1 h; (c) DMAP (0.2 equiv), Et_3N (1.5 equiv), Ac_2O (1.9 equiv), DMF, 80 °C, 24 h, 69–76%.

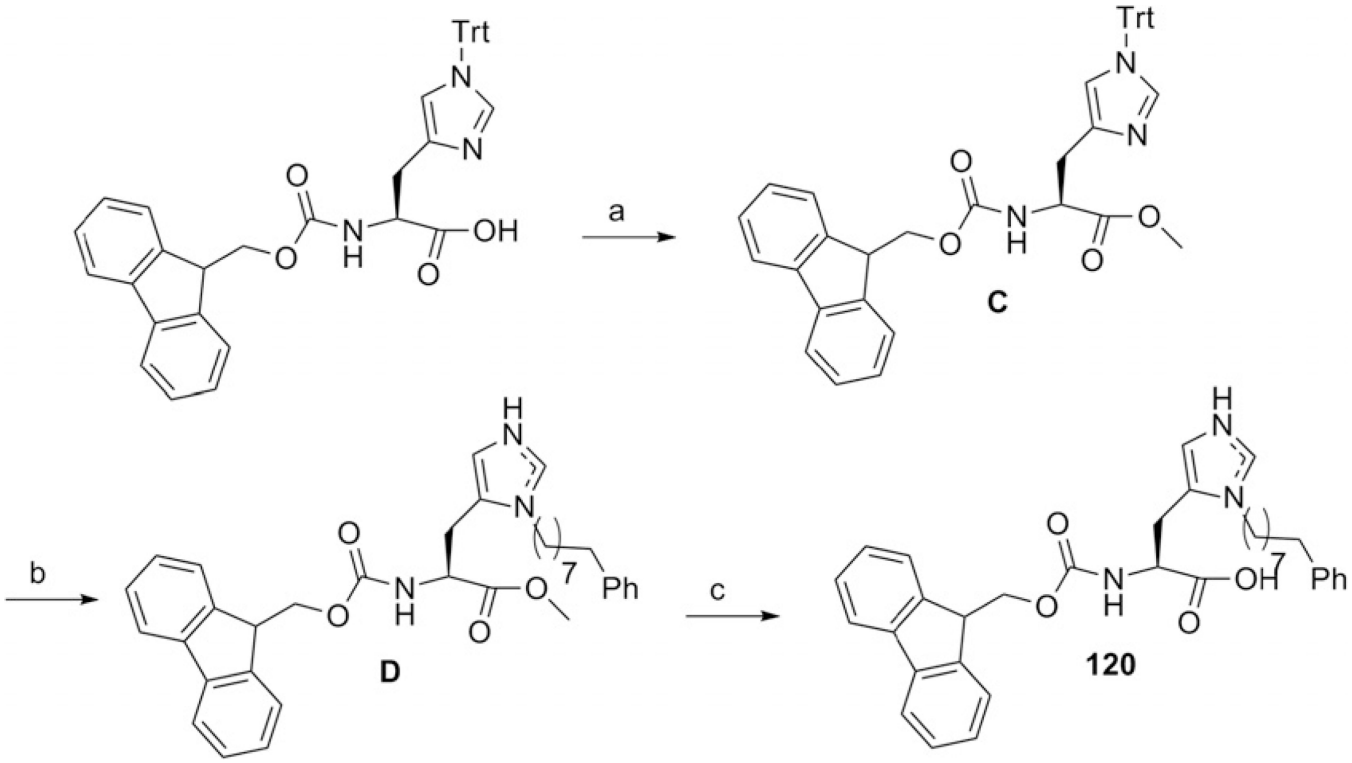

Scheme 5.

Reagents and conditions: (a) HOBt (1.5 equiv), DCC (1.5 equiv), THF, rt, overnight, quan; (b) (1) Tf_2O (1.1 equiv), 8-phenyl-1-octanol (1.1 equiv), DIEA (1.1 equiv), CH_2Cl_2, —75 °C to rt, 16 h; (2) TFA (10 equiv), TIPS (1.1 equiv), CH_2Cl_2, rt, 2 h, quan for two steps; (c) 2 N HCl/1,4-dioxane (v/v, 1/1), 100 °C, 3 h, 64%.